Experimental Validation of Model of Electro-Chemical-Mechanical Planarization (ECMP) of Copper

J. L. Ebert*, S. Ghosal, D. de Roover, and A. Emami-Naeini
SC Solutions, Inc.
*Corresponding author: SC Solutions, Inc., 1261 Oakmead Pkwy, Sunnyvale, CA 94085. jle@scsolutions.com

Abstract: This paper describes the development of a COMSOL model of Electro-Chemical-Mechanical Planarization (ECMP) that was validated with experimental data. ECMP is an emerging technology for processing of semiconductor wafers. We developed a 2D model of flow of phosphoric acid solution (the electrolyte) between two parallel plates, the top plate representing the pad and the bottom plate representing the wafer. By using this relatively simple geometry, we were able to focus on the physics and electrochemistry in ECMP. The model includes steady-state copper dissolution and species transport inside the electrolyte, ion transport including convection, diffusion, and migration, and electrodic reactions represented by the Butler-Volmer equation. An experimental set-up for validating this ECMP model was fabricated, and experiments were conducted to measure the anode current was measured at various spatial locations for different electrode potentials. The results of the experiment and the COMSOL model were found to be in very good agreement.

Keywords: ECMP, Electro-Chemical-Mechanical-Planarization, electropolishing.

1 Introduction

The goal of this work has been the development of an experimentally-validated model of the Electro-Chemical-Mechanical Planarization (ECMP) process using COMSOL Multiphysics. ECMP [1], [2] is used for semiconductor fabrication for planarizing (polishing) wafers, and is considered to be particularly suited to planarizing low-k interconnects at technology nodes of 32 nm and below. The ECMP polishing technique uses electrochemical etching and gentle mechanical action to remove copper atoms, and has a very low down-force that minimizes potential for damage that is associated with conventional CMP. A schematic of a generic ECMP system is shown in **Figure 1**. While there are simulation results from simple electrical models (without electrochemistry) reported in the literature [3], we were not able to find any studies involving detailed, physics-based models of the ECMP process similar to the one described in this paper.

The COMSOL model of electrochemistry and species transport predicts the dependence of the removal rate on other process parameters such as electrolyte concentration and applied voltages. The 2D model comprises of phosphoric acid solution (the electrolyte) flowing between two parallel plates representing the pad and the wafer as shown in **Figure 2**. The pad moves with a constant velocity with respect to the reference frame of the wafer. The flow velocity profile in the gap is linear at steady-state. The wafer surface is the working electrode and is held at a constant potential V_a, and is coated with a film of copper that would be removed using ECMP. The copper film is sufficiently thick that we can ignore potential drops through the film. Use of a relatively simple geometry, allowed us to focus on the transport and electrochemistry processes involved in ECMP. The model includes steady-state copper dissolution and species transport inside the electrolyte, ion transport including convection, diffusion, and migration, and electrodic reactions represented by the Butler-Volmer equation. It computes the steady-state copper dissolution current density as a function of the voltage applied $V_e = (V_a - V_c)$.

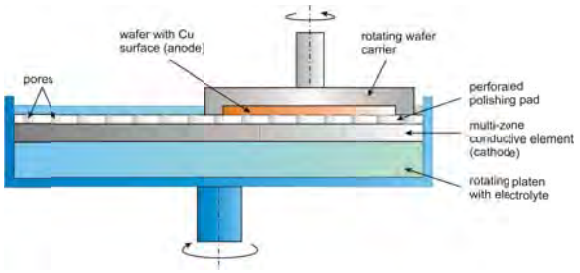

Figure 1: Schematic of ECMP system.

An experimental set-up for validating the ECMP model was fabricated, and experiments were conducted to measure the anode current was measured at various spatial locations for different electrode potentials. The experimental apparatus consisted of a two-zone counter-electrode in the form of approximately one-half of a cylinder, and a working electrode that consists of a whole cylinder. The working electrode rotates near the stationary two-zone counter-electrodes. The space between electrodes was either electrolyte or a pad material. A probe was embedded into the working electrode to

measure the local current density. This probe consisted of a copper wire installed perpendicular to the curved surface of the cylinder. Using a circuit, we maintained the probe at ground while measuring the small electrical currents through the wire. The working electrode was also at ground while the counter-electrode voltages were varied as desired. As the working electrode and probe rotated, we recorded the probe current as a function of angle.

The results of the experiment and the COMSOL model are in very good agreement. We concluded that the validated COMSOL model was ready for use in model-based control of the ECMP process.

2 ECMP Model Development

2.1 Theory of Electrolytic Removal of Copper

In this section, we describe the physics and chemistry underlying the COMSOL FEM model that was developed to simulate the electrochemical removal of copper from a surface. The system under consideration consists of two parallel plates of length L separated by a distance H as shown in **Figure 2**. One plate is a wafer surface coated with a film of copper (Cu) that we want to remove. This wafer surface is the *working electrode* and is held at a constant potential V_a. The Cu film is sufficiently thick that we can ignore potential drops through the film. The other plate (the *counter-electrode*) is at potential V_c. The flow between the plates consists of a solution of phosphoric acid (H_3PO_4) and water. The rotational motion of the polishing pad is represented by motion of the pad surface in the x direction, which results in a linear velocity profile in the vertical direction, $u(y)$.

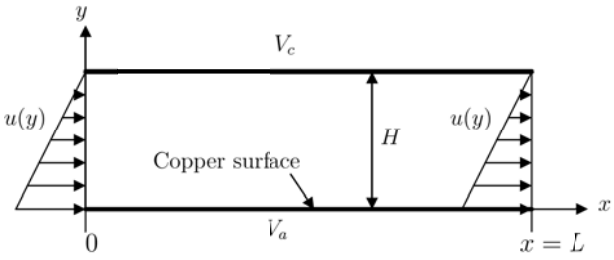

Figure 2: Schematic of the geometry used for COMSOL model development.

We assume the acid dissociates in the solution according to the following reaction to form the hydronium ion, H_3O^+.

$$H_3PO_4 + H_2O \rightleftharpoons H_2PO_4^- + H_3O^+. \quad (1)$$

The value equilibrium constant K_a is 7.25×10^{-3}, and the forward reaction rate, K_f is 1.3×10^{-4}, both at 25°C [1]. The backward reaction rate, K_b, is hence (K_f/K_a), i.e., 1.79×10^{-2}. The forward and backward rate constants are used to estimate the concentrations of $H_2PO_4^-$ and H_3O^+ as shown later (Eq. 6). In using concentration in place of *activity* with rate constants, we assume a standard concentration of c_{std} = 1 mol/l and normalize concentrations using c_{std}. Effectively, this means we need to use units of mol/l for all concentration ratios involved with chemical reactions. For phosphoric acid with density of 1700 kg/m^3 and molecular weight, M_{H3PO4} = 98 g/mol, we have a concentration of approximately $[H_3PO_4^-]$ = 17 mol/l.

We can estimate the electrical conductivity, k, of this solution using the following relationship:

$$k = \frac{F^2}{RT}\sum_i z_i^2 D_i C_i \quad (2)$$

In reality, k decreases at high ionic concentrations when the mobility is more complex [6]. For our model, however, we will ignore these effects and assume D_i is constant and use k from Eq. 2.

The species flux is the sum of the electromigration, diffusive and convective fluxes [6], [7]:

$$\mathbf{N}_i = \underbrace{-z_i u_i F c_i \nabla\Phi}_{\text{migration}} \underbrace{- D_i \nabla c_i}_{\text{diffusion}} \underbrace{+ c_i \mathbf{v}}_{\text{convection}}. \quad (3)$$

flux

Here, $\mathbf{N}_i$ is the flux density of species i, mol/m^{2}s, z_i is the number of proton charges on ion, e.g., z_{Cu2+} = 2, u_i is the mobility of species i ($u_i = D_i/RT$), F is the Faraday's constant, 96,500 C/mol of charge, D_i is the diffusion coefficient for species i, (m^2/s), c_i is the concentration of species i, (mol/m^3), and $\mathbf{v}$ is the velocity vector (in m/s). The current density in the electrolyte is given by

$$\mathbf{i} = F\sum_i z_i \mathbf{N}_i. \quad (4)$$

The species conservation equation is

$$\frac{\partial c_i}{\partial t} = -\nabla\cdot\mathbf{N}_i + R_i. \quad (5)$$

Here, R_i is the volumetric production of species i. For our model, R_i is non-zero only for the hydronium ion, and is governed by the forward and backward reaction rate constants (k_f and k_b, respectively).

$$R = k_f[H_3PO_4][H_2O] - k_b[H_2PO_4^-][H_3O^+]. \quad (6)$$

The net charge in the electrolyte is zero, outside the tiny (un-modeled) double layers near electrodes.

$$\sum_i z_i c_i = 0. \quad (7)$$

If we rewrite the current density expression (Eq. 4) by substituting for flux density (Eq. 3) then we obtain:

$$\mathbf{i} = -F^2\nabla\Phi\sum_i z_i^2 u_i c_i - F\sum_i z_i D_i \nabla C_i + FV\sum_i z_i c_i. \quad (8)$$

The last term of Eq. 8 is zero in the electrolyte due to charge neutrality since the flow field does not carry current [7]. The first term is regular electrical conduction where electrical conductivity is given by:

$$\kappa = F^2 \sum_i z_i^2 u_i c_i. \quad (9)$$

Both positive and negative charges increase the conductivity since the charge is squared, i.e., z_i^2. Additionally, current is generated as a result of potential gradients (charge migration) or from concentration gradients (species diffusion), and the current density can be expressed as:

$$\mathbf{i} = -\kappa \nabla \Phi - F \sum_i z_i D_i \nabla c_i. \quad (10)$$

Imposing the charge neutrality condition, $\sum z_i c_i = 0$, also implies that $\sum z_i \nabla c_i = 0$. Thus, it is noted that differences in diffusivity (D_i) is key to whether the species concentrations term affects current flow. If all the diffusivities were identical, the second term in Eq. 10 would be zero.

A voltage drop across the electrodes drives the following chemical reaction at the anode, resulting in the formation of a positively charged copper-water complex, $Cu(H_2O)_6^{2+}$ [4], [5]:

$$Cu(s) + 6H_2O \rightleftharpoons [Cu(H_2O)_6]^{2+} + 2e^-. \quad (11)$$

A *double-layer*, which may be as thin as a few nanometers, will form at the surface of each electrode with a significant voltage drop across it. Consequently, enormous electric fields exist across this very thin double-layer. For our modeling purposes, we can ignore changes over the length scales of the double layer and simply treat it as a boundary condition. The concentrations of the four species of interest are denoted as follows:

$$c_1 = [H_2O]; \quad c_2 = [Cu(H_2O)_6^{2+}];$$

$$c_3 = [H_3O^+]; \quad c_4 = [H_2PO_4^-].$$

We use the Nernst equation to compute the zero-current equilibrium potential across the double-layer:

$$E = E^0 - \frac{RT}{nF} \log\left(\frac{c_2}{c_1^6}\right). \quad (12)$$

Here, T = 298 K, RT/F = 26 mV, and n=2 is the number of electrons in the reaction and E^0 is the standard electrode potential. This potential is relative to a Standard Hydrogen Electrode (SHE) so that E^0=0.34V for this Cu^{2+} reaction. This equation shows that if we increase the copper or decrease the water at the surface the equilibrium potential will drop.

If we drive the electrode with a potential higher than E then we will drive current out of the electrode, into the electrolyte, and out through the cathode. The relationship that governs this current flow is the Butler-Volmer equation:

$$i = i_0 \left[\exp\left(\frac{\alpha_a F}{RT}\eta_s\right) - \exp\left(\frac{\alpha_c F}{RT}\eta_s\right)\right]. \quad (13)$$

Here, $\eta_s = V_a - E$ is defined as the surface *overpotential*. As we drive copper to the cathode, the same reaction (in reverse) will take place and the similar equations will be used to compute the potential drop across the double-layer. Typically the constants α_a and α_c are approximately equal, with the constraint that $\alpha_a + \alpha_c = n$. For the copper reaction near room temperature, the exchange current density, i_0 = 10 A/m^2, α_a = 1.5, and α_c = 0.5 [6].

So Eq. 13 gives us a surface current for a given overpotential η_s. When $\eta_s = 0$ the current goes to zero. We can use this directly as a flux boundary condition because to convert from a current density to species density we divide by zF, where z is the charge of the ion - here z = 2. Thus, the flux of c_2 into the electrolyte at the surface is:

$$\mathbf{N}_2 \cdot \hat{y} = \frac{i_o}{zF}\left[\exp\left(\frac{\alpha_a F}{RT}\eta_s\right) - \exp\left(-\frac{\alpha_c F}{RT}\eta_s\right)\right]. \quad (14)$$

We note that Eq. 11 is actually a combination of two reactions – one that generates Cu^{2+} at the surface, and another that forms a complex with the copper atom and six water molecules that is carried into the electrolyte [5]. Consequently, from flux balance, the flux of H_2O into the electrolyte at the surface is given by $\mathbf{N}_1 \cdot \hat{y} = -6\mathbf{N}_2 \cdot \hat{y}$.

Some of the reports in the literature assume that the overpotential, η_s, has a large positive value on one electrode (e.g., the anode) and has a large negative at the other electrode (e.g., the cathode). In such cases, one may ignore one of the two terms in Eq. 13, and obtain the Tafel equation. However, if one runs the overpotential to near zero, this approximation may result in significant errors. Also, if one uses a segmented "electrode" that can be driven with a voltage distribution then this anode/cathode terminology can be tricky. It may be more useful to consider α_a and α_c as properties at surfaces that depend on the specific local chemistry. If the chemistry changes along a given surface the constants α's may change as well.

The current flow in the electrolyte is due to the potential gradient in the electrolyte (migration) and also due to concentration gradients (diffusion) as described by Eq. 10. To determine the potential Φ within the electrolyte, we apply the current conservation equation: $\nabla \cdot \mathbf{i} = 0$, and obtain:

$$\nabla \cdot \left[-\kappa \nabla \Phi - F \sum_i z_i D_i \nabla c_i \right] = 0. \quad (15)$$

The boundary values for the potentials are the equilibrium potentials E computed at each location on the surface from the Nernst equation, Eq. 12.

The schematic in **Figure 3** shows a typical potential drop across the electrolyte. We assume that the anode (bottom) is at a voltage of V_a and the cathode (top) is at a voltage of V_c. From the local surface concentrations we compute the equilibrium potentials E_a and E_c at the anode and cathode. Since these concentrations will vary along the surfaces, so will the equilibrium potentials. Then at each surface location we compute the overpotential $\eta_s = V_a - E$ and use the Butler-Volmer equation (Eq. 13 or 14) to compute the surface species flux (or current). The ohmic contribution to the potential drop across the cell ($\nabla\Phi$) may be small, depending on the electrolyte conductivity and over-voltage values. Also, due to the cross-flow, it is unlikely that the profile of the voltage drop will be a linear as shown, but would decrease in the direction of current flow.

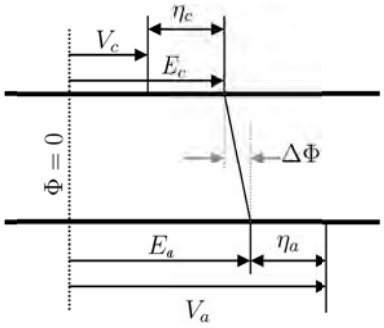

Figure 3: Potential distribution across the cell.

The species concentrations $c_1, \ldots, c_4$ have to be first determined in order to compute the electrical conductivity of the electrolyte (Eq. 2). The concentrations of water (c_1) and copper complex (c_2) are computed using species conservation $\nabla \cdot \mathbf{N}_i = 0$ where we assume the absence of homogeneous reactions (R) and a steady-state process. The concentrations of the two charged species, $c_3 = [H_3O^+]$ and $c_4 = [H_2PO_4^-]$ are computed using charge conservation (Eq. 7) and the H_3PO_4 equilibrium dissociation constant, i.e., we assume there is ample phosphoric acid and it dissociates fast compared to our fluxes.

We further assume that the concentration of phosphoric acid is constant and is denoted by c_0. Then $c_3.c_4 = c_0$, and the charge neutrality condition yields $z_1c_1 + z_2c_2 + z_3c_3 + z_4c_4 = 0$. Substituting $z_1=0$, $z_2=2$, $z_3=1$, $z_4=-1$ gives $2c_2+c_3-c_4=0$. Solving these two equations, we obtain:

$$c_3 = -c_2 + \sqrt{c_2^{\,2} + c_0}, \qquad c_4 = \frac{c_0}{c_3}. \qquad (16)$$

2.2 Implementation in COMSOL and Simulation Results

We used COMSOL Multiphysics' PDE (General Form) interface to implement the model, together with the Electric Current interface. **Figure 4** shows the FEM geometry with the electrolyte flowing between the two plates separated by H = 2.92 mm. The electrolyte flow enters from the left boundary and exits through the right boundary. The electrolyte flow velocity is specified to increase linearly from the counter-electrode to the anode, the latter moving to the right with a velocity U_0 (= 6 mm/s).

The species fluxes (Eq. 3) for water, copper-water complex, $Cu(H_2O)_6^{2+}$, and the hydronium ion, H_3O^+, were specified under the Conservative Flux field in the General Form PDE interface, and the production of H_3O^+ was specified under Source Term. Concentrations of the three species at the entrance boundary were specified using Constraint interface, as was the flux balance between copper and $Cu(H_2O)_6^{2+}$ at the anode. The concentrations of $Cu(H_2O)_6^{2+}$ and H_3O^+ were specified as zero at the counter electrode. The Flux/Source interface was used to specify the flux of $Cu(H_2O)_6^{2+}$ at the anode using the Butler-Volmer equation. The Flux/Source interface was also used to specify the convective flux of the three species at the exit.

The electrical conductivity of the medium (Eq. 9) was specified in the Electric Currents interface under Current Conservation. The contribution to the current density in both x and y directions by the diffusion of charged species was specified under External Current Density interface. The voltage at the cathode (counter-electrode), –0.8 V, was specified using Electrical Potential interface. The segment of the counter-electrode to the right was grounded (V_2 = 0), and effectively served as a second anode with the boundary condition specified using the Ground interface. As described later, this segmented electrode configuration was used in the experiment to study the current distribution in the region at the boundary of the two segments. The diffusivities of the four species H_2O, $Cu(H_2O)_6^{2+}$, H_3O^{+}-, and $H_2PO_4^-$ (c_1–c_4) used in the model are 5.0×10^{-9} m^2/s, 1.4×10^{-9} m^2/s, 3×10^{-9} m^2/s, and 0.9×10^{-9} m^2/s, respectively [8].

Figure 5 shows that H_3O^+ is present in equilibrium concentrations in most of the electrolyte except near the electrodes. At the anodes, water depletion results in H_3O^+ depletion and at the cathode, the ion gives up the positive charge to the electrode. This behavior is also seen in the

concentration profile of H_3O^+ in the y-direction in the graphs of **Figure 6**. The species boundary layer for $Cu(H_2O)_6^{2+}$ is shown on the left graph, while the concentration of $H_2PO_4^-$, computed using charge balance of Eq. 16, is shown on the right of **Figure 6**. **Figure 7** (left) shows the copper removal rate that was computed from the gradient of the copper complex flux, $\frac{\partial c_2}{\partial y}$, at the anode, or alternatively from Eq. 14. The removal rate decreases in the direction of the flow as less water is available to create the copper complex, and finally falling to zero at the end of the anode. The graph on the right side of **Figure 7** shows that the current density at the counter electrode (cathode) drops quickly to a uniform value over the length of the electrode.

3 Experimental Validation

3.1 Experimental Apparatus and Procedure

An experiment was done to validate the detailed electrochemical model. The apparatus was as shown in **Figure 8**(a) consisting of a cylindrical copper electrode (anode) and two adjacent partial cylindrical electrodes (Electrode 1 and 2). The central rotating electrode, the anode, was made from a copper cylinder with diameter approximately 32 mm. A small hole was drilled into the cylinder wall (1.2 mm) and an insulated wire (approx. 1.06 mm in diameter) was placed flush with the hole. The insulated wire acted as a probe that measured the current distribution as the anode sweeps past the cathode. The anode and probe are both held at ground, but the current through the probe is measured using the inverting amplified circuit shown in **Figure 8**(b). We note that this experimental configuration is well approximated by the 2D because *H* is much smaller than the radius of the cylindrical counter electrode used in the experiment.

For all of these validation experiments Electrode 2 was maintained at ground (V = 0), and hence acted essentially as an additional anode. The voltage on Electrode 1 was varied from zero to –3 V using a Hewlett Packard E3615A DC power supply. The current was measured through Electrode 1 using a shunt resister. For most the results shown here, the probe amplifier resistor was R = 2.0 kΩ, resulting in an amplifier gain of 2000.

Figure 9 shows a photograph of the assembled apparatus. The rotation was controlled with a servo motor and servo motor controller (located at the top of the assembly), and the speed could be adjusted manually. For the results shown here, the anode surface speed was approximately 6.3 mm/s. A position sensor was constructed by removing the housing from a 10 kW potentiometer. This allowed the potentiometer sweep arm to rotate freely and by applying a constant voltage across the potentiometer the sweep voltage could be measured to determine angular position.

To connect the probe to the probe amplifier, a rotating electrical contact made of graphite was constructed using a copper cylinder that was electrically insulated from the rotating shaft. At the bottom of the assembly are the rotating anode and the stationary counter electrodes. The position of the counter electrodes relative to the rotating anode could be adjusted using the three electrode alignment rods. Once the assembly had been aligned, the whole set-up could be raised and lowered with the release knob so that the bottom end could be inserted into a container of electrolyte.

The electrolyte used was 85% phosphoric acid (H_3PO_4) and the container held approximately 100 ml of acid. It was determined that one had to replace the electrolyte fairly regularly since the etched copper would remain in the electrolyte so results would drift with time. After approximately an hour of polishing (depending on the rate) the electrolyte would start to take on a green tint, and the currents would start to diminish.

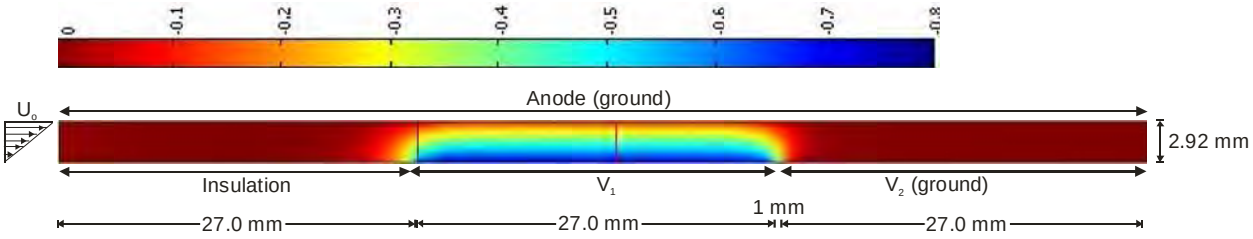

Figure 4: 2D COMSOL model for ECMP. The electrolyte flow enters from the left. Polishing occurs at the copper anode (top "wall") which is moving at velocity U_0 with respect to the bottom "wall". There is 1 mm gap of insulation between the segmented counter-electrodes at voltages V_1 and V_2.

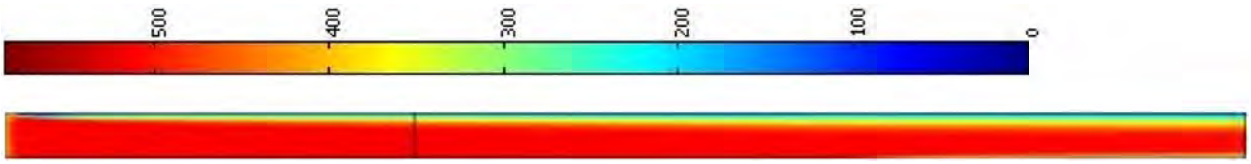

Figure 5: Distribution of the hydronium ion, H_3O^+, concentration (moles/m^3) throughout the electrolyte.

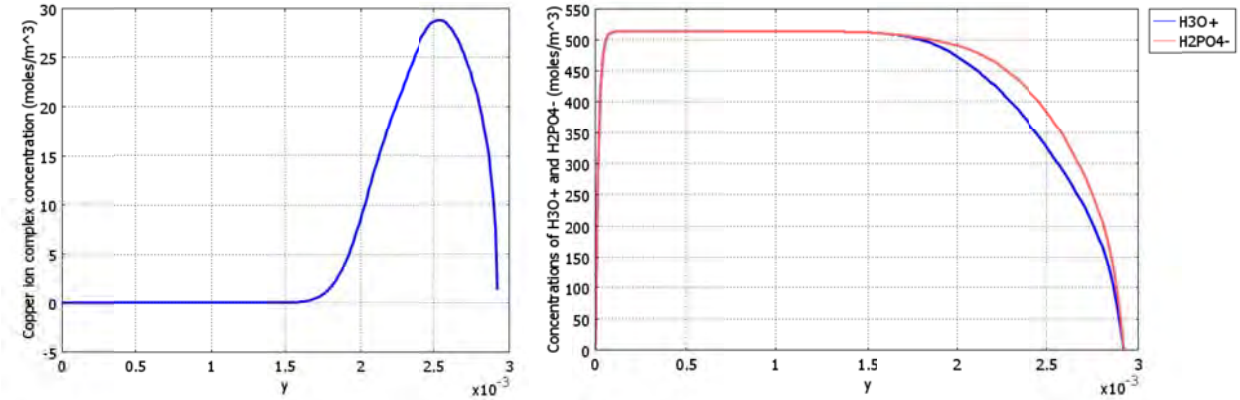

Figure 6: Left: Molar concentration of $Cu(H_2O)_6^{2+}$ in the vertical (y) direction at x = 0.015 m (shown as the vertical line in Figure 5). **Right:** $H_2PO_4^-$ and H_3O^+ molar concentrations.

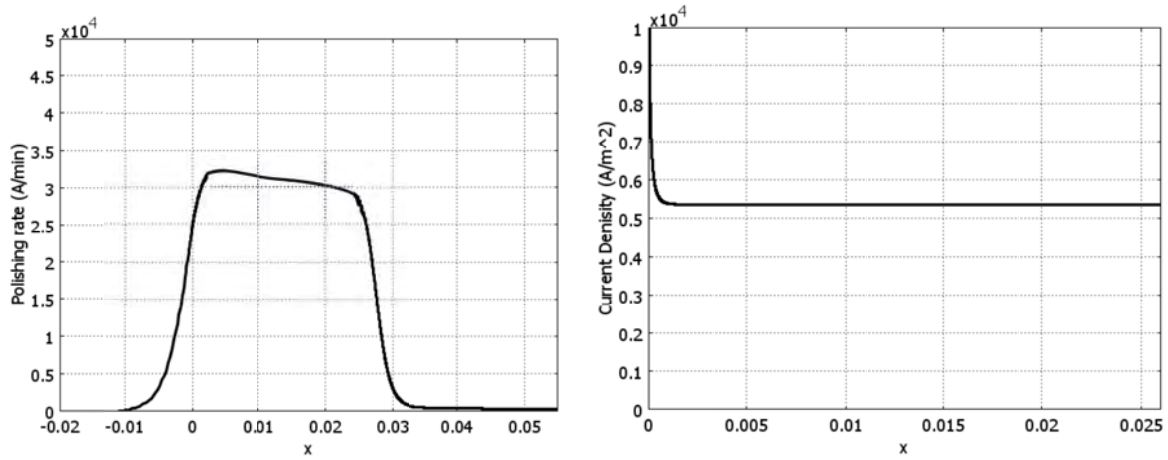

Figure 7: Left: Copper polish rates in A/min at the anode. **Right:** Current density at the counter electrode.

3.2 Experimental Results

Figure 10 shows the measured current *vs*. voltage graph. The current starts to rise as the voltage from the anode to cathode increases above 0.5 V. After the voltage exceeds approximately 1.0 V, we start to see a noisier signal. This is due to the formation of bubbles of hydrogen (H_2) at the cathode. At 1.4 V, the current increase is large and the gas evolution at the cathode is fairly vigorous. At voltages above approximately 1.4 V further voltage increase does not increase current very much, and the noise due to gas evolution is significantly large.

Figure 11 shows the probe current for the case where the voltage between the electrodes was approximately 0.8 V. The dots are data and the red line is the results from the COMSOL model. The vertical scale of the plot is in the units determined experimentally, but the model results were scaled by a constant factor to match the values at the peak current. Additionally, we used a scaling factor for the inflow concentration of H_2PO_4 since there was some uncertainty in the actual concentration. Nevertheless, the characteristics are clearly the same. As the probe sweeps from left to right (increasing position) we see the current suddenly rise within approximately 5-6 mm range. After the peak, the current decreases gradually with increasing position due to thickening of the Cu ion diffusion boundary layer. The current drops off suddenly as the probe exits the Electrode 1 area. As can be expected, the shape of the graph is very similar to the copper flux from the anode shown in **Figure 7**.

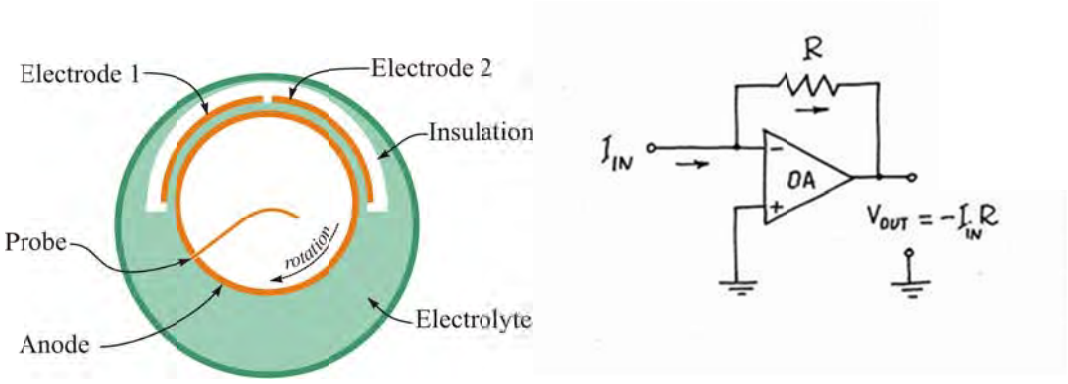

(a) (b)

Figure 8: Left: Schematic of experimental apparatus (top view). **Right: C**ircuit for measuring probe current while maintaining probe at V=0.

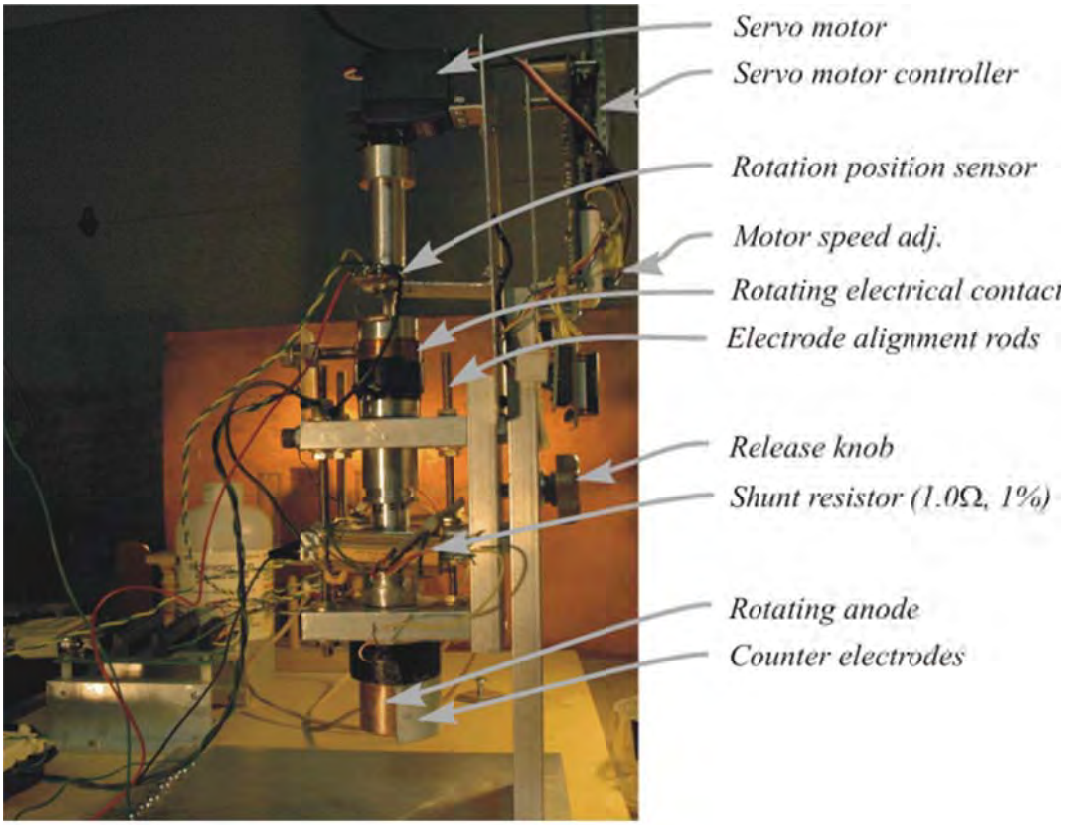

Figure 9: Apparatus for conducting the ECMP experiments.

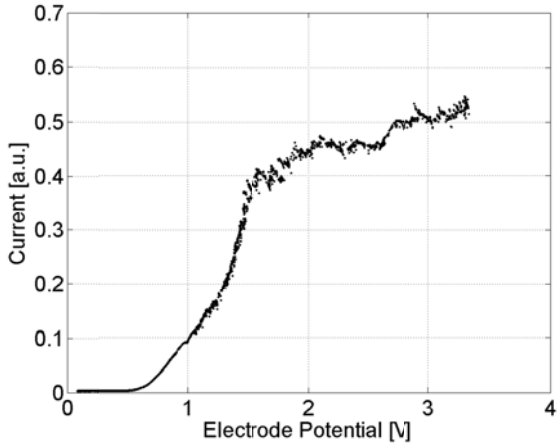

Figure 10: Electrode 1 current *versus* voltage from anode to cathode.

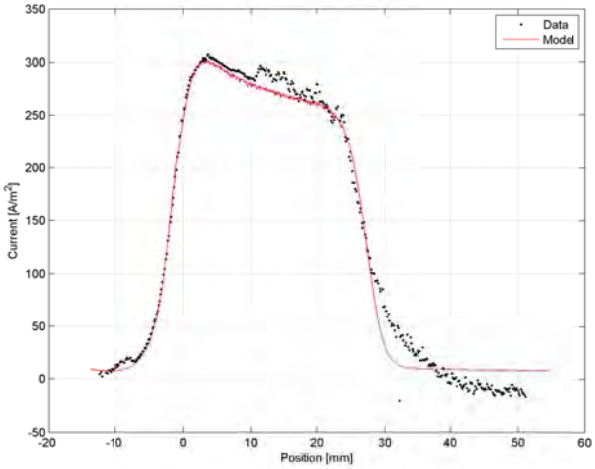

Figure 11: Comparison of anode current data with COMSOL model predictions.

4 Conclusions

We have developed a steady-state COMSOL model of the ECMP process that includes copper dissolution and species transport inside the electrolyte, ion transport including convection, diffusion, and migration, and electrodic reactions represented by the Butler-Volmer equation. The removal rate and uniformity are predicted as a function of electrolyte concentration and applied voltage. An experimental apparatus was built, and a series of successful experiments were carried out. Our experimental results show excellent agreement with the COMSOL model predictions. A reduced-order version of the validated physical model may now be used as a basis for developing multivariable feedback control of the ECMP process.

5 References

[1] *Microelectronic Applications of Chemical Mechanical Planarization*, Ed. Y. Li, Wiley-Interscience, (2008).

[2] D. Padhi, J. Yahalom, S. Gandikota, and G. Dixit, "Planarization of Copper Thin Films by Electropolishing in Phosphoric Acid for ULSI Applications," *J. Electrochem. Soc.*, **Vol. 150**, No.1, pp. G10-G14, (2003).

[3] D. Truque, X. Xie, and D. Boning, "Wafer Level Modelling of Electrochemical-Mechanical polishing (ECMP)," *Mater. Res. Soc. Symp.*, **Vol. 991**, (2007).

[4] R. Vidal and A. C. West, "Copper Electropolishing in Concentrated Phosphoric Acid. I. Experimental Findings," *J. of Electrochem. Soc.*, **Vol. 142**, No. 8, pp. 2682-2689, (1995).

[5] R. Vidal and A. C. West, "Copper Electropolishing in Concentrated Phosphoric Acid II: Theoretical Interpretation," *J. Electrochem. Soc.*, **Vol. 142**, No. 8, pp. 2689-2694, (1995).

[6] G. Prentice, *Electrochemical Engineering Principles*, (1991).

[7] J. Newman and K. E. Thomas-Alyea, *Electrochemical Systems*, 3rd ed., (2004).

[8] *CRC Handbook of Chemistry and Physics*, 74th ed., (1994).

6 Acknowledgements

This work was funded by the NSF SBIR Program, Award # IIP-0740214. We gratefully acknowledge the help of Professor Jan B. Talbot of the University of California, San Diego (UCSD) Department of Nano-engineering during the course of this research.